Research Journal of Recent Sciences _____ ISSN 2277-2502
Vol. **2(4),** 1-10, April **(2013)** *Res. J. Recent Sci.*

Study on the Inhibition of Mild Steel Corrosion by Quaternary Ammonium Compound in H_2SO_4 Medium

Prathibha B.S.[1], Kotteeswaran P.[2] and Bheema Raju V.[3],
[1]Department of Chemistry, BNM Institute of Technology, Bengaluru-70, INDIA
[2]Department of Chemistry, Kalasalingam University, Tamil Nadu, INDIA
[3]Department of Chemistry, Dr. Ambedkar Institute of Technology, Bengaluru, INDIA

Available online at: www.isca.in
Received 28th August 2012, revised 8th January 2013, accepted 12th February 2013

Abstract

The inhibition effect of Tetra-n-butylammonium bromide (TBAB) on the corrosion of mild steel in Sulphuric acid was investigated. The corrosion inhibiting action was studied through weight loss, polarization and electrochemical impedance spectroscopy techniques. The surface characterization was done by scanning electron microscopy. The polarization experiment reveals that the studied inhibitor acts as mixed type inhibitor. The %IE increases with increase in concentration but decreases with increase in temperature .Langmuir adsorption isotherm fits the experimental data for the studied compound. Thermodynamic and kinetic parameters are evaluated.SEM study provide the confirmatory evidence for the protection of mild steel by the studied inhibitor.

Keywords: Mild steel, SEM, inhibitor, quaternary ammonium compound.

Introduction

Mild steel is one of the industrially important metals and is inevitable to expose its surface to the different industrial environments while in use. The steel undergoes corrosion to different extent depending on the aggressiveness of the medium or environment. Generally the service life of steel is enhanced by applying various corrosion control measures. Most of the available methods for controlling corrosion are based on modifying either the surface of the metal or local environment when the metal is exposed. In most of the industries like oil refineries, nuclear power plants, fertilizer and chemical etc. the steel is used as containers, steam generators, liquid carrying pipes and so on. In such cases the corrosion of steel is effectively controlled by the application of suitable inhibitors. Most of the acid corrosion inhibitors are organic compounds, such as those containing N, S, O and aromatic ring. Sulphur and nitrogen containing compounds have been found to be effective corrosion inhibitors. Most of the organic inhibitors act by adsorption on the metal surface. The adsorption of organic inhibitors at metal/solution interface can markedly change the corrosion resisting properties of metals. The protection of corroding surfaces prevents the waste of both resources and money during the industrial applications and it is vital for the extension of the life time of the equipment and limiting dissolution of toxic metals from components into environment.

It has been reported that quaternary ammonium compounds are important as inhibitor additives in hydrochloric acid and sulphuric acids. The effect of concentrations, functional groups and halide ions of quaternary ammonium inhibitors on the corrosion of iron and steel have been studied extensively. The synergistic effect between the organic cations and the halide anions is considered to be an important factor in inhibiting action on metal corrosion[1,2]. As a representative type of these organic inhibitors, quaternary ammonium salts have been demonstrated to be highly cost-effective and used widely in various industrial processing for preventing corrosion of mild steel in acidic medium. Literature revealed that long chain n-alkyl quaternary ammonium compounds act as good corrosion inhibitors. Meakins has reported that N-alkyl quaternary ammonium compounds inhibit the corrosion of mild steel in acids and the effectiveness of the inhibitor increases regularly with an increase in alkyl chain length.

In the present work the inhibition of corrosion of mild steel in 0.5M H_2SO_4 in the presence of Tetra-n- - butylammonium bromide has been evaluated at different temperatures and at different concentrations of inhibitor using weight loss, Tafel polarization and Electrochemical impedance measurements. Kinetic and thermodynamic properties of this compound was studied. The relationship between these properties and the inhibitive efficiency of the corrosion inhibitor are discussed.

Experimental

Preparation of the specimen: Mild steel specimens (Fe, 98.7; C, 0.223; Mn, 0.505; Si, 0.164; S, 0.05.) of dimension 2cm x1cm were polished to a mirror finish, degreased with acetone and alcohol followed by double distilled water, and used for the weight loss method and surface examination studies.

Weight loss method: Mild steel specimens, in triplicate, were immersed in 100ml of the solutions containing various

concentrations of the inhibitors for 3h. The weight of the specimens before and after immersion was determined using electronic balance. The corrosion rate was calculated using the formula

$$C.R(mm/y) = \frac{87.6W}{DAT} \quad (1)$$

Where W= weight loss in mg, D = density of mild steel in g/cm^3, A = area of the specimen in square centemeter , T = Time of exposure in hours

Electrochemical experiment: Electrochemical experiments were performed in a conventional three electrode cell, mild steel welded with copper wire and embedded in Teflon holder using epoxy resin with an exposed area 1cm^2 as Working electrode, a platinum foil of 1cm^2 was used as counter electrode and the reference electrode was a saturated calomel electrode (SCE) with a Luggin capillary. All potentials are measured with respect to the SCE. Measurements were performed using CHI 660C model electrochemical workstation.

Potentiodynamic polarization curves were obtained by scanning the potential range from -200mv + E_{corr} to +200 mv + E_{corr} at a scan rate of 10mV/s after 1h immersion time in 1M HCl and 1M HCl + inhibitor solutions.

Electrochemical impedance measurements were carried out at open – circuit potential over a frequency range of 0.01Hz – 100 KHz. The sinusoidal potential perturbation was 10mv in amplitude. Electrochemical data were obtained after 1h of immersion with the working electrode at the rest potential and all tests have been performed in non-deaerated solutions under stirred conditions. Potentiodynamic polarization curves were also obtained at different temperatures to calculate the activation energy of the inhibitor adsorption to mild steel surface.

Surface examination study: The mild steel specimens were immersed in the absence and presence of optimum concentration of inhibitor in 0.5M H_2SO_4 for a period of 3h. After 3h the specimen were taken out and dried. Surface analysis was done with scanning electron microscopy.

Results and Discussion

Weight- loss method: The inhibition efficiencies (IE) and corrosion rate as determined by the weight loss test of mild steel in 0.5M H_2SO_4 in the temperature range 298 K – 328K with and without the addition of different concentration of the inhibitor is given in the table 1. The figure 1 shows that the %IE increases with concentration and Figure 2 shows that the inhibition efficiency decreases with increase in temperature.

Potentiodynamic polarization: The polarization of curves of mild steel in the absence and presence of different concentration of inhibitors at different temperatures are shown in Figure 3. The Various corrosion parameters such as corrosion potential (E_{corr}), corrosion current density (i_{corr}), Anodic(b_a) and cathodic (b_c) Tafel slopes and percentage inhibition efficiency (%IE_2) for studied inhibitor are given in table 2. The corrosion current densities were determined from the intersection by extrapolating the cathodic and anodic Tafel lines. Tables 2 show the variation of E_{corr} values with the concentration of studied inhibitors in 0.5M H_2SO_4. The corrosion potential shifts to a positive potential with respect to the Blank but the displacement in corrosion potential is less than 35mv in studied inhibitor, according to Ferreira and W.H. Li if the displacement in corrosion potential is more than 85mv with respect to the corrosion potential of the blank, the inhibitor can be seen as a cathodic or anodic type[3,4]. The maximum displacement was <35mv which indicated that the studied quaternary ammonium compounds acts as mixed type inhibitor[4]. It is also observed from the table that both the anodic and cathodic slopes changes which thereby suggesting that the studied inhibitors acts as mixed type inhibitor. As can be seen from these polarization results, the corrosion current density decreases with increase in concentration for all studied inhibitors, thus the inhibition efficiency increases with increase in concentration. Table 2 revealed that the corrosion current density increases with temperature thus %IE decreases with increase in temperature.

Electrochemical impedance spectroscopy: Inhibition efficiencies and other calculated impedance parameters are given in table 3. When the inhibitor concentration increases, C_{dl} values tend to decrease. It can be attributed to the decrease in local dielectric constant or increase in thickness of surface film layer by the adsorption of the inhibitor molecules on the metal solution interface. The value of R_{ct} is a measure of the electron transfer across the surface and is inversely proportional to corrosion rate. R_{ct} increases with increase in concentration. The semicircle shaped Nquist plots shown in figure 4 indicate the formation of a barrier on the surface and a charge transfer process mainly controlling the corrosion of MS. The values of n_{dl} related to $(CPE)_{dl}$ are found in the 0.78-0.82 interval indicating the electrode surface are partially heterogeneous[5].

Thermodynamic parameters and Adsorption isotherms: Adsorption isotherms are very important in determining the mechanism of organic electrochemical reactions. Various adsorption isotherms were tested but Langmuir adsorption isotherms found to be best fit for the studied quaternary ammonium compound. The Langmuir adsorption isotherm is given by the following equation

$$\frac{C}{\theta} = \frac{1}{K} + C \quad (2)$$

Where C is the inhibitor concentration and K is equilibrium constant of adsorption, which is related to standard free energy of adsorption ΔG^0_{ads} by:

$$K = \frac{1}{55.55} \exp\left(\frac{-\Delta G^0_{ads}}{RT}\right) \quad (3)$$

ΔG^0_{ads} is obtained at a given temperature. K is obtained from the intercept of a plot of C/Θ as a function of C. As seen from the figure 5, plot of C/Θ as a function of C yields a straight line

with regression co-efficient higher than 0.99, showing that the adsorption of the inhibitor is fitted to Langmuir adsorption isotherm.

The data reported in the table 4 reveals that, the adsorptive equilibrium constant (K) decreases with increasing the temperature indicating that it is easy for inhibitor to adsorb on to the mild steel surface at relatively low temperature, but as the temperature increases, the adsorbed inhibitor tends to desorb. These results suggest that, the inhibition of mild steel is a adsorptive process. This isotherm assumes that the adsorbed molecules occupy only one site and there are no interactions between the adsorbed species[6].

Thermodynamic parameters play an important role in understanding the inhibition mechanism. The enthalpy of adsorption and entropy of adsorption are calculated from the following equations

$$\log\left(\frac{\theta}{1-\theta}\right) = \log A + \log C_{inh} - \frac{Q_{ads}}{2.303RT} \quad (4)$$

Where A is a constant, and Q_{ads} is the heat of adsorption equal to enthalpy of adsorption enthalpy of adsorption (ΔH^0_{ads}) is obtained from the slope of a plot of $\log\left(\frac{\theta}{1-\theta}\right)$ vs 1/T at various concentrations.

The entropy of activation (ΔS^0_{ads}) is obtained from the equation :

$$\Delta G^0_{ads} = \Delta H^0_{ads} - T\,\Delta S^0_{ads} \quad (5)$$

Figure 6 indicates that there is a good linear relationship between $\log\left(\frac{\theta}{1-\theta}\right)$ and 1/T . The negative sign of ΔG^0_{ads}

Indicates that the inhibitor is spontaneously adsorbed on the metal surface [6]. Generally, the magnitude of ΔG^0_{ads} around -20kJ/mol or less negative, leads to the assumption that an electrostatic interaction exists between the inhibitor and the charged metal surface i.e. physisorption. Standard free energy of adsorption around -40kJ/mol or more negative indicates that a charge sharing or transferring from organic species to the metal surface occurs to form a coordinate type of bond i.e. chemisorptions[7].

In the present study, the ΔG^0_{ads} values obtained ranges from -24.1 to -26.4 kJ/mol, which are lower than -40 kJ/mol but higher than -20 kJ/mol. This indicates that the adsorption is neither typical physisorption nor typical chemisorptions but it is complex mixed type. That is the adsorption inhibitor molecules on the mild steel surface in the present study involves both physisorption and chemisorptions (comprehensive adsorption) but physisorption is the predominant mode of adsorption. This assumption is supported by the data obtained from temperature dependence of inhibition process, reported in table 2, which shows that the inhibition efficiency of the studied quaternary compound decreases with increase in temperature (Physisorption)[8].

As for the value of ΔH^0_{ads} in Table 4 , the sign of ΔH^0_{ads} is negative indicates the exothermic nature of steel dissolution process. The negative sign of ΔS^0_{ads} which indicates that an increase in ordering takes place in going from reactants to metal-adsorbed species reaction complex[9].

Kinetic parameters: The adsorption phenomena have been explained by using thermodynamic parameters, to further elucidate the inhibition properties of the inhibitor, the kinetic model was employed. The kinetic parameters for the corrosion process were calculated from Arrhenius equation and the transition state equation:

$$i_{corr} = A\exp\frac{-E_a}{RT} \quad (6)$$

Where i_{corr} is the corrosion current density, A is the Arrhenius constant, E_a is the activation energy and R is the universal gas constant.

$$i_{corr} = \frac{RT}{Nh}\exp\left(\frac{\Delta S^*}{R}\right)\exp\left(\frac{-\Delta H^*}{RT}\right) \quad (7)$$

Where N is Avogadro's constant, h is planck's constant, ΔS^* is the change in entropy of activation and ΔH^* is the change in enthalpy of activation.

E_a is obtained from the slope of a plot of $\ln(i_{corr})$ vs 1/T (Figure 7), ΔS^* is obtained from the intercept of a plot of $\log\left(\frac{i_{corr}}{T}\right)$ vs 1/T and ΔH^* is obtained from the slope of a plot of $\log\left(\frac{i_{corr}}{T}\right)$ vs 1/T (figure 8).

The kinetic parameters calculated are given in table 5. It is clear from that table 5 that the E_a increased with increasing concentration of studied inhibitor. Also it is clear that E_a values in the presence of inhibitor are higher than that in the absence of inhibitor indicating higher activation energies for the metal dissolution reaction. Hence the process is activation controlled. The increase in apparent activation energy E_a may be interpreted as physical adsorption [10]. Szauer and Brand explained that the increase in activation energy can be attributed to an appreciable decrease in the adsorption of the inhibitor on the mild steel surface with increase in temperature and a corresponding increase in corrosion rates occurs due to the fact that greater area of metal is exposed to the acidic solution environment [11]. The positive sign of enthalpy of activation reflect the endothermic nature of steel dissolution process meaning that dissolution of steel is difficult. It is clear from the table 5 that the entropy of activation is large and negative imply that the activated complex in the rate determining step represents an association rather than dissociation step, meaning that a decrease in disordering take place on going from reactant to the activated complex[12,13].

Table-1
Inhibition efficiency of various concentrations of TBAB for the corrosion of mild steel in 0.5MH_2SO_4 by weight loss method at different temperatures (298K-328K)

	Temperature							
	298		308		318		328	
Inhibitor concentration (M)	**%IE**	**Corrosion rate(mm/y)**	**%IE**	**Corrosion rate(mm/y)**	**%IE**	**Corrosion rate(mm/y)**	**%IE**	**Corrosion rate(mm/y)**
Blank		59.88		112.89		225.8		410.1
1 X 10^{-3}	**40.9**	35.33	**20.5**	89.64	**18.8**	183.4	**10.2**	368.2
2 X 10^{-3}	**46.9**	31.80	**32.1**	76.63	**29.3**	159.6	**15.4**	346.8
4 X 10^{-3}	**52.5**	28.45	**48.2**	58.40	**37.7**	140.6	**28.7**	292.5
6 X 10^{-3}	**60.5**	23.62	**53.5**	52.45	**43.2**	128.1	**36.5**	260.4
1 X 10^{-2}	**68.9**	18.59	**60.6**	44.45	**57.2**	96.53	**50.2**	204.2

Table-2
Electrochemical Polarization parameters for MS in 0.5MH_2SO_4 Containing different concentrations of TBAB at different temperatures

Concentration(M)	**E_{corr} (mV)**	**i_{corr} (µA/cm^2)**	**b_a (mV/decade)**	**b_c (mV/decade)**	**IE(%)**
298K					
Blank	-502.8	5997	159.5	162.6	
1x 10^{-3}	-469.9	2940	125.9	168.3	50.9
2 x 10^{-3}	-463.3	2363	118.7	175.3	52.3
4 x 10^{-3}	-457.3	1925	112.3	171.4	60.9
6 x 10^{-3}	-451.0	1401	104.6	166.7	67.9
1 x 10^{-2}	-447.8	154.9	97.7	154.9	76.6
308K					
Blank	-497.1	10530	189.4	186.9	
1x 10^{-3}	-466.0	7738	149.3	177.8	26.5
2 x 10^{-3}	-466.0	5976	141.5	174.0	43.2
4 x 10^{-3}	-473.2	4556	127.4	174.8	56.7
6 x 10^{-3}	-477.1	4185	119.9	166.2	60.2
1 x 10^{-2}	-489.0	3109	103.4	156.3	70.5
318K					
Blank	-495.4	18910	203.9	201.9	
1x 10^{-3}	-458.5	14710	169.6	182.7	22.2
2 x 10^{-3}	-454.5	12340	165.5	173.0	34.7
4 x 10^{-3}	-455.3	10180	153.1	176.4	46.2
6 x 10^{-3}	-460.4	8192	143.1	179.1	56.7
1 x 10^{-2}	-470.0	5921	127.7	171.2	68.7
328K					
Blank	-485.9	27230	196.2	201.1	
1x 10^{-3}	-461.4	24070	204.2	210.0	11.6
2 x 10^{-3}	-453.8	21840	179.1	200.6	19.8
4 x 10^{-3}	-444.1	17210	171.9	174.1	36.8
6 x 10^{-3}	-447.9	14050	156.9	171.0	48.4
1 x 10^{-2}	-454.0	9634	143.2	175.8	64.6

Table 3
Impedance parameters of mild steel in 0.5MH_2SO_4 absence and presence of different concentration of TBAB at 25^{0}C

Concentration (M)	Y_{dl} (Ω^{-1} cm^{-2} S^{ndl} 10^{-4})	n_{dl}	R_{ct} (Ω)	C_{dl} ($\mu F/cm^2$)	IE (%)
0.5M H_2SO_4	15.39	0.8657	5.016	723.6	
1 x 10^{-3}	22.44	0.8221	8.50	952.6	**40.9**
2 x 10^{-3}	21.04	0.8027	9.80	810.4	**48.8**
4 x 10^{-3}	19.9	0.8017	11.11	775.1	**55.0**
6 x 10^{-3}	18.76	0.796	14.34	742.7	**65.0**
1 x 10^{-2}	16.93	0.7855	18.75	659.9	**73.2**

Table-4
Thermodynamic parameters obtained from adsorption isotherms for TBAB in 0.5M H_2SO_4

Temperature (K)	R	Slope	K_{ads}	ΔG^0_{ads} (kJmol^{-1})	ΔH_{ads} (kJ/mol)	ΔS_{ads} (J/mol/K)
298	0.9954	1.2086	775.2	-26.4	-37.1	-17.8
308	0.9982	1.1853	404.8	-25.6	-37.1	-19.8
318	0.9961	1.1133	271.0	-25.4	-37.1	-19.8
328	0.9933	0.7251	122.5	-24.1	-37.1	-23.2

Table-5
Corrosion kinetic parameters for mild steel in 0.5M H_2SO_4 in absence and presence of different concentrations of TBAB

Concentration (M)	E_a (kJ/mol)	$\Delta H^{\neq}$ (kJ/mol)	$\Delta S^{\neq}$ (J/mol/K^{-1})
Blank	42.6	39.9	-155.3
1 x 10^{-3}	53.4	50.8	-110.4
2 x 10^{-3}	55.2	52.8	-114.8
4 x 10^{-3}	56.2	53.5	-118.4
6 x 10^{-3}	56.7	54.1	-122.2
1 x 10^{-2}	57.8	55.1	-131.3

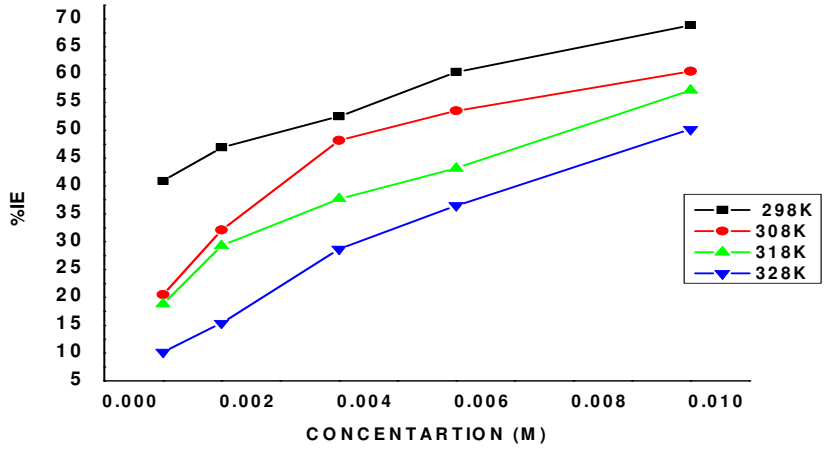

Figure-1
Variation of %IE with concentration obtained from weight loss method

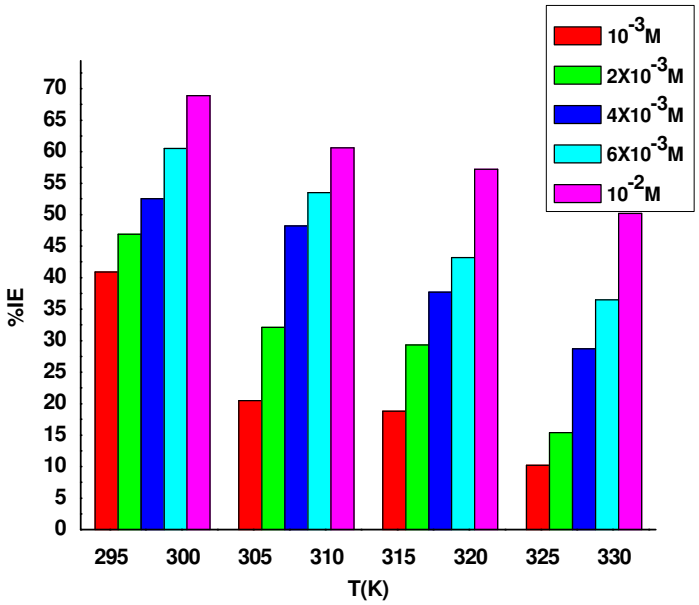

Figure-2
Variation of %IE with temperature for different concentration of TBAB

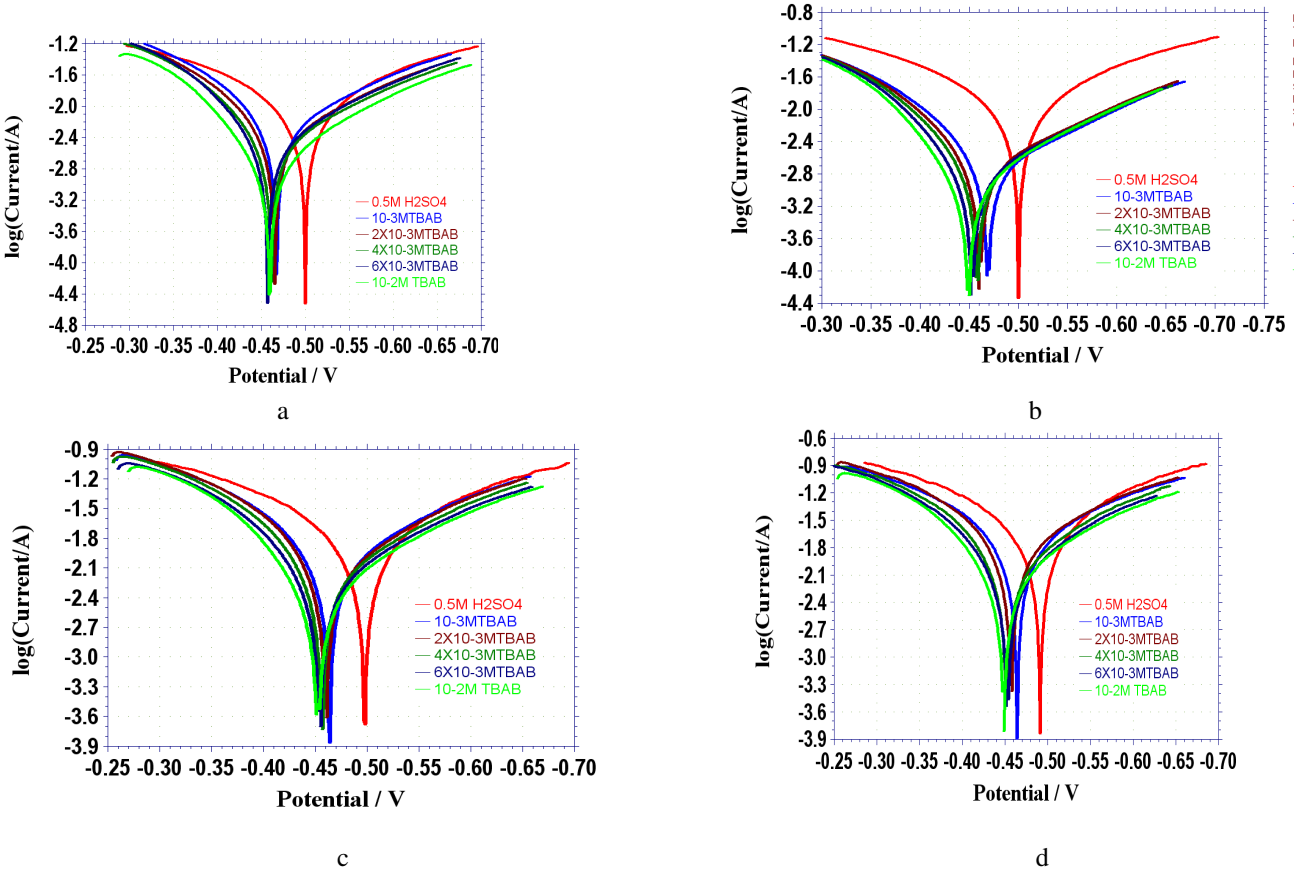

Figure-3
Typical Tafel plots of MS in 0.5MH_2SO_4 in presence and absence of different concentration of TBAB at a) 25^{O}C b) 35^{O}C c) 45^{O}C and d) 55^{O}C

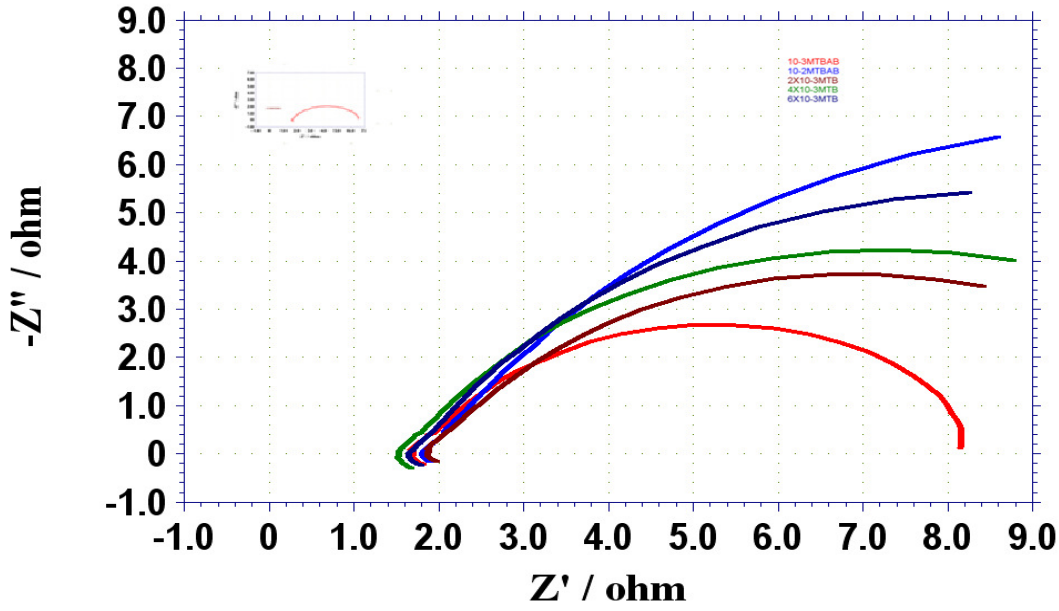

Figure-4
Nyquist Plots of mild steel in 0.5MH_2SO_4 absence and presence of TBAB

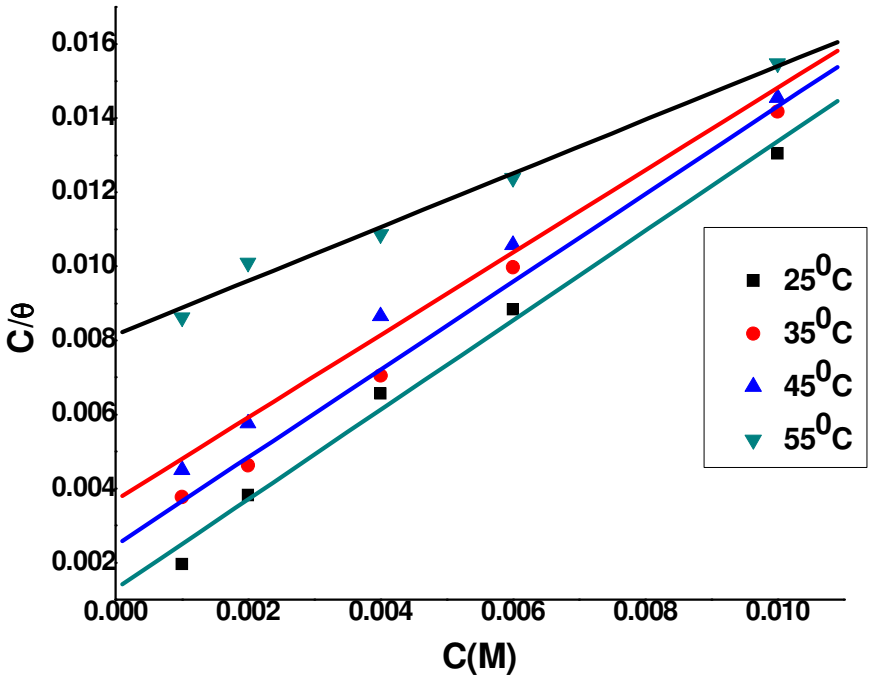

Figure-5
Langmuir adsorption isotherms of TBAB at different temperatures

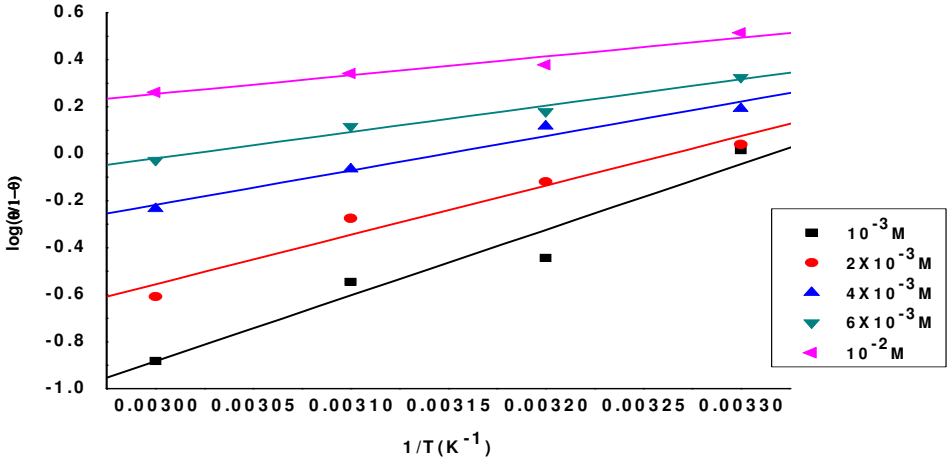

Figure-6
Variation of $\log\left(\frac{\theta}{1-\theta}\right)$ vs 1/T

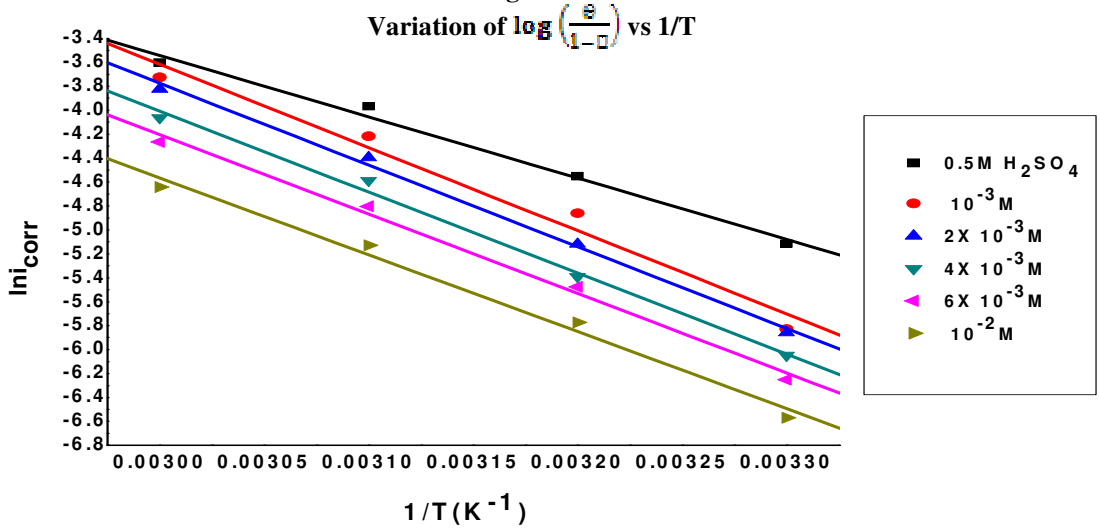

Figure-7
Arrhenius plots for mild steel in 0.5MH_2SO_4 without and with various concentration of TBAB

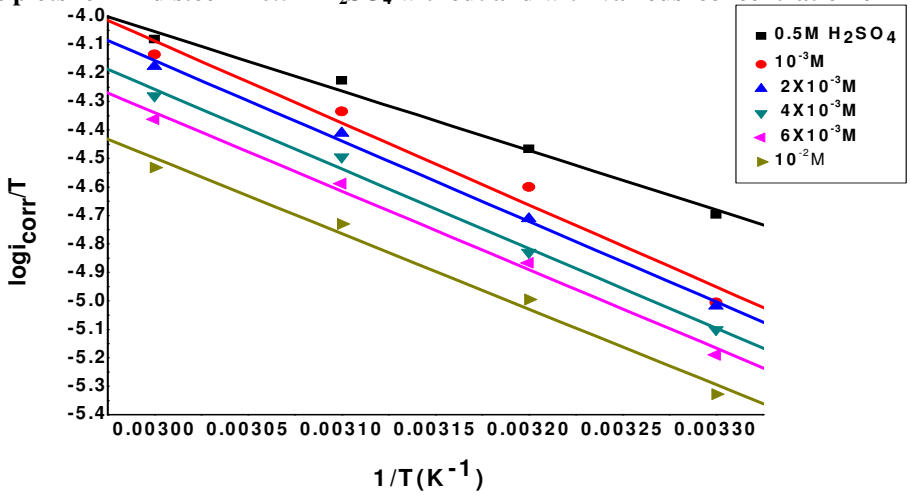

Figure-8
Transition state plots for mild steel in 0.5MH_2SO_4 without and with various concentration of TBAB

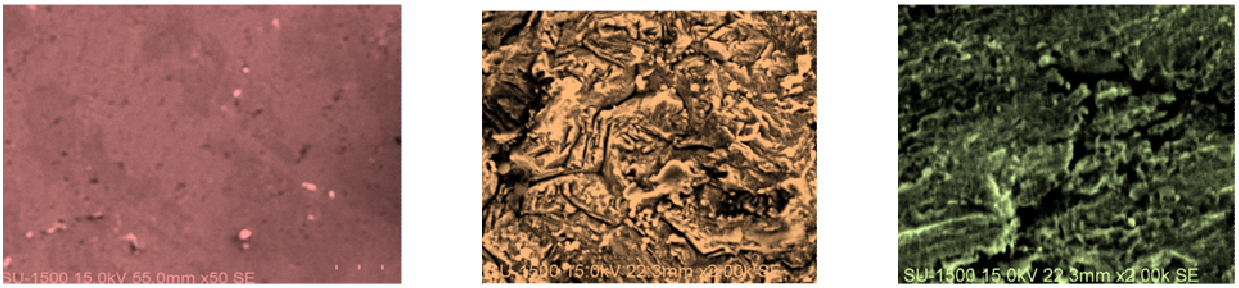

a b c

Figure-9
Surface Characterization by SEM for mild steel in 0.5M H_2SO_4 a) Polished surface b) in the absence of inhibitor c) in the presence of TBAB

SEM Analysis: The surface morphology of mild steel was studied by scanning electron microscopy, surface was observed after 3h of immersion in the absence and presence of Inhibitor. Figure 9a,b and c shows the SEM images for polished surface, in the absence of inhibitor and in the presence of inhibitor respectively. Figure 9b shows that the surface was severely damaged in the absence of inhibitor. Figure 9c shows the steel surface protected after adding optimum concentration of inhibitor.

Mechanism of Adsorption: According to the mechanism for the anodic dissolution of Fe in acidic sulphate solutions proposed initially by Bockris et al, Fe electro-dissolution in acidic sulphate solutions depends primarily on the adsorbed intermediate $FeOH_{ads}$ as follows [14] :

$Fe + H_2O \leftrightarrow [FeOH]_{ads} + H^+ + e$
$[FeOH]_{ads} \rightarrow [FeOH]^+ + e$ (rate determining step)
$[FeOH]^+ + H^+ \rightarrow Fe^{+2} + H_2O$

The cathodic hydrogen evolution follows the steps:

$Fe + H^+ \leftrightarrow (FeH^+)_{ads}$
$(FeH^+)_{ads} + e \leftrightarrow (FeH)_{ads}$
$(FeH)_{ads} + H^+ + e \rightarrow Fe + H_2$

The corrosion rate of iron in H_2SO_4 solutions is controlled by the hydrogen evolution reaction and dissolution reaction of iron.

The inhibition process, from a theoretical standpoint, has been regarded as a simple substitution process, in which an inhibitor molecule(I) in the aqueous phase substitutes an x number of water molecules adsorbed on the surface[15-17]:

$I (aq) + xH_2O \leftrightarrow I_{ads} + xH_2O (aq)$

In the presence of halide ions(X^{-1}), the mechanism for the anodic dissolution is given as [17, 18].

$Fe + H_2O + X^- \leftrightarrow [FeXOH]^-_{ads} + H^+ + e$
$[FeXOH]^-_{ads} \rightarrow FeXOH + e$ (rate determining step)
$FeXOH + H^+ \rightarrow Fe^{+2} + X^- + H_2O$

The process of adsorption is influenced by the nature and charge of the metal, chemical structure of inhibitor and the type of aggressive electrolyte. The charge of the metal surface can be determined from the potential of zero charge (PZC) on the correlative scale ($Ø_c$) by the equation

$Ø_c = E_{corr} - E_{q=0}$

Where $E_{q=0}$ is the potential of the zero charge. However, a value obtained in H_2SO_4 is -502.8 mv vs SCE. The PZC of iron is -550mV in H_2SO_4, therefore $Ø_c$ is positive (+47.2) and hence the mild steel surface acquires positive charge. In strong acid solution, studied inhibitors, ionizes and carry a positive charge. As Steel surface is positively charged in presence of H_2S0_4 medium, while Bromide ion is negatively charged, as a result the specific adsorption of bromide ion occurs onto mild steel surface, causing negatively charged surface of steel. By means of electrostatic attraction, Quaternary ammonium cation easily reaches mild steel surface, so bromide ion acts as an adsorption mediator for bonding metal surface and inhibitor. This gives rise to the formation of an adsorption composite film in which Br^{-1} ion are sandwiched between metal and positively charged part of inhibitor. This film acts as a barrier facing corrosion process.

Conclusion

The inhibition efficiency of studied inhibitor increases with increasing the inhibitor concentration but decreases with increasing temperature. The adsorption of the Tetra-n-butylammonium bromide obeys Langmuir adsorption isotherm. The adsorption process is spontaneous and exothermic process accompanied by decrease of entropy. E_a is more for the inhibited solution compared to that of the uninhibited solution. Potentiodynamic polarization curves revealed that the studied inhibitor acts as a mixed type inhibitor.

Acknowledgement

I thank Roop Singh, general manager, SINSIL International, Bangalore for extending the electrochemical characterization facility.

References

1 Soror T.Y., and El-Ziady M.A., Effect of cetyl trimethyl ammonium bromide on the corrosion of carbon steel in acids, *Mater. Chem. Phys.*, **77(3)**, 697-703 **(2003)**

2 Caliskan N. and Bilgic S., Effect of iodide ions on the synergistic inhibition of the corrosion of manganese-14 steel in acidic media, *Appl. Surf. Sci*., **153(2-3)**, 128-133 **(2000)**

3 Ferreira E.S., Giacomelli C., Giacomelli F.C. and Spinelli A., Evaluation of the inhibitor effect of L-ascorbic acid on the corrosion of mild steel, *Mater. Chem. Phys*., **83(1)**, 129-134 **(2004)**

4 Li W.H., He Q., Pei C.L. and Hou B.R., Some new triazole derivatives as inhibitor of mild steel corrosion in acidic medium, *J. Appl. Electrochem.*, **38(3)**, 289-295 **(2008)**

5 Singh D.D.N. and Dey A.K., Synergitic effects of inorganic and organic cations on inhibitive performance of propargyl alcohol on steel dissolution in boiling hydrochloric acid solution, *Corros*., **49(7)**, 594-600 **(1993)**

6 Avci G., Corrosion inhibition of indole-3-acetic acid on mild steel in 0.5M HCl, *Colloids Surf.,* **317(1-3)**, 730-736 **(2008)**

7 Benali O., Larabi L., Traisnel M., Gengembra L. and Harek Y., Electrochemical, theoretical and XPS studies of 2-mercapto-1-methylimidazole adsorption on carbon steel in 1M $HClO_4$, *Appl. Surf. Sci.,* **253(14)**, 6130-6139 **(2007)**

8 Solomon M.M., Umoren S.A., Udosoro I.I and Udoh A.P., inhibitive and adsorption behavior of carboxymethyl cellulose on mild steel corrosion in sulphuric acid solution, *Corros. Sci.,* **52(4)**, 1317-1325 **(2010)**

9 Banerjee G. and Malhotra S.N., Contribution to adsorption of aromatic amines on mild steel surface from HCl solutions by impedance, UV and Raman spectroscopy, *Corrosion*, **48(1)**, 10-15 **(1992)**

10 El Sherbini E.E.F., Effect of some ethoxylated fatty acids on the corrosion behavior of mild steel in sulphuric acid solution, *Mater. Chem. Phys*., **60(3)**, 286-290 **(1999)**

11 Szauer T. and Brand A., On the role of fatty acid in adsorption and corrosion inhibition of iron by amine-fatty acid salts in acidic solution, *Electrochim. Acta*, **26(9)**, 1257-1260 **(1981)**

12 Marsh J., Advanced organic chemistry, Wiley Eastern 3rd edition, **(1988)**

13 Bentiss F., Lebrini M. and Lagrenee M., Thermodynamic characterization of mild steel dissolution and inhibitor adsorption processes in mild steel /2,5-bis(n-thienly)1,3,4-thiadiazoles/ hydrochloric acid system, *Corros. Sci*., **47(12)**, 2915-2931 **(2005)**

14 Bockris J.O.M., Drazic D. and Despic A.R., The electrode kinetics of the deposition and dissolution of iron, *Electrochim. Acta*, **4(2-4)**, 325-361 **(1961)**

15 Ateya B.G., El-Anadouli B.E. and El-Nizamy F.M., The adsorption of thiourea on mild steel, *Corros. Sci.*, **24(6)**, 509-515 **(1984)**

16 El-Awady A.A., B.A. Abd-El-Nabey and S.G. Aziz, Kinetic –thermodynamic adsorption isotherms analyses for the inhibition of the acid corrosion of steel by cyclic and open-chain amines, *J. Electrochem. Soc*., **139(8)**, 2149-2154 **(1992)**

17 Chin R.J. and Nobe K., Electrodissolution kinetics of iron in chloride solutions, III. Acidic solutions, *J. Electrochem Soc.,* **119(11)**, 1457-1461 **(1972)**

18 MacFarlane D.R. and Smedley S.I., The dissolution mechanism of iron in chloride solutions, *J. Electrochem. Soc*., **133(11)**, 2240-2244 **(1986)**